

On the Plants Leaves Boundary, “Jupe à Godets” and Conformal Embeddings

Sergei Nechaev^{†‡1}, Raphaël Voituriez^{†2}

[†] *Laboratoire de Physique Théorique et Modèles Statistiques, Université Paris Sud,
91405 Orsay Cedex, France*

[‡] *L D Landau Institute for Theoretical Physics, 117940, Moscow, Russia*

The stable profile of the boundary of a plant’s leaf fluctuating in the direction transversal to the leaf’s surface is described in the framework of a model called a “surface à godets”. It is shown that the information on the profile is encoded in the Jacobian of a conformal mapping (the coefficient of deformation) corresponding to an isometric embedding of a uniform Cayley tree into the 3D Euclidean space. The geometric characteristics of the leaf’s boundary (like the perimeter and the height) are calculated. In addition a symbolic language allowing to investigate statistical properties of a “surface à godets” with annealed random defects of curvature of density q is developed. It is found that at $q = 1$ the surface exhibits a phase transition with the critical exponent $\alpha = \frac{1}{2}$ from the exponentially growing to the flat structure.

key words: isometric embedding, tellesation, conformal transform, graph of the group

PACS: 02.40.-k; 87.17.Ee

¹ E-mail: nechaev@ipno.in2p3.fr

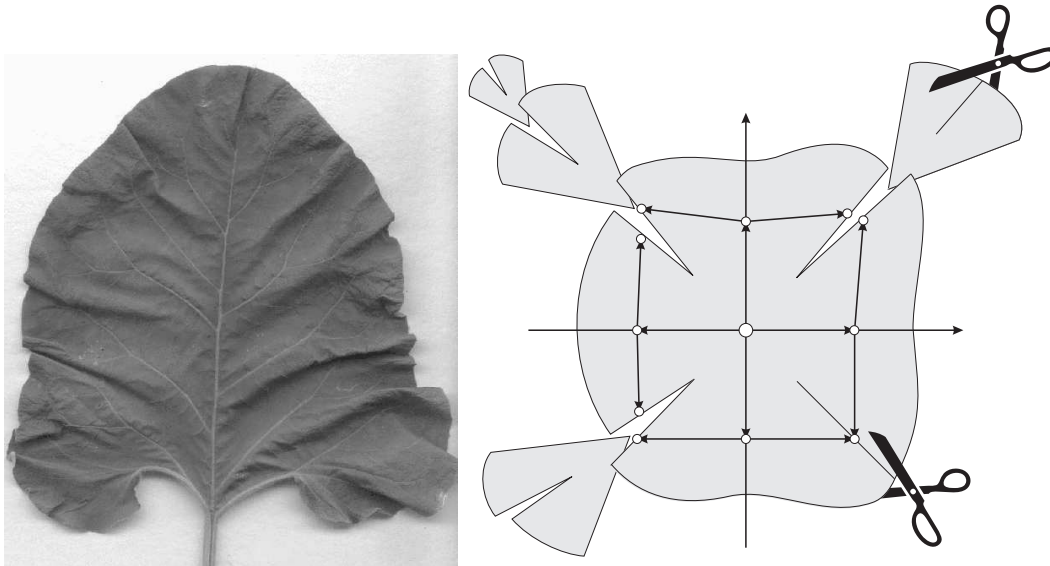
² E-mail: voiturie@ipno.in2p3.fr

I. INTRODUCTION

The very subject of this paper has been inspired by the following questions raised by V.E.Zakharov in a private conversation about two years ago: (1) "What are the geometrical reasons for the boundary of plants leaves to fluctuate in the direction transversal to the leaf's surface?" and (2) "How to describe the corresponding stable profile?" The answer to question (1) has come immediately.

It is reasonable to imagine that cells located near the leaf's boundary proliferate more active than ones in the bulk of the leaf. One possible reason might be purely geometric: the periphery cells are not completely enclosed by the surrounding media and hence have more available space for growth than the cells inside the leaf's body*. The corresponding picture of the burdock leaf (*arctium lappa*) is reproduced in fig.1a. This phenomenon can be observed for various species such as most of types of lettuce (*lactuca sativa*) or spinach (*spinacea oleracea*)... The schematic model of the suggested geometric origin of the leaf's folding is shown in fig.1b (see the explanations below).

At the same time the question (2) remained unanswered, and in this paper we discuss some possible ways of solution to this problem. Relying on the growth mechanism of a plant's leaf conjectured above, one can propose the following naive construction schematically shown in fig.1b. Take some "elementary" bounded domain of a flat surface, make finite radial cuts and insert in these cuts flat triangles, modeling the area newly generated by periphery cells. The resulting surface obtained by putting back together all elementary domains and inserted extra triangles is not flat anymore. Continue the process recursively, i.e. make cuts in the new surface, insert extra flat triangles and so on... One gets this way a surface whose perimeter and area grow exponentially with the radius. Several examples can be found in [1].



*Despite this explanation seems rather natural, some biological justifications of the expressed hypothesis would be worthwhile.

FIG. 1. (a) Picture of a burdock’s leaf (*Arctium lappa*), (b) The surface à godets isometrically covered by a 4–branching Cayley tree.

Apparently a similar problem had been discussed for the first time by the Russian mathematician P.L.Tchebychef in his talk ”On the cut of clothes” in Paris on 28 August 1878, apparently unpublished (some traces of this talk we found in the web page [2]). Among the modern developments of that subject one can mention the paper [3] by P.Bowers proving in 1997 the theorem on quasi–isometric embedding of a uniform binary tree into a negatively curved space, as well as the contribution [4] by S.Duval and M.Tajine devoted to isometric embeddings of trees into metric spaces for fractal description.

Our forthcoming consideration is based on two suppositions: (i) the plant’s leaf has infinitesimal thickness without any surface tension, and (ii) activity of boundary cells is independent on the size of the leaf.

The surface constructed above is called ”hyperbolic” [5]. Anyone who pays attention to the tendencies in fashion recognizes in this recursive construction the so–called ”jupe à godets”. Later on we shall call such surfaces the ”surfaces à godets”. Despite this rather transparent geometrical image, the very problem under consideration is still too vague. Let us formulate it in more rigorous terms, which allow the forthcoming mathematical analysis.

Let us cover the surface à godets by a natural ”lattice”. The construction of this ”lattice” is as follows. Take a 4–branching Cayley tree[†]. It is well known that any regular Cayley tree, as an exponentially growing structure, cannot be isometrically embedded in any space with flat metric. One can expect that the ”surface à godets”, being by construction an exponentially growing (i.e. ”hyperbolic”) structure, admits Cayley trees as possible discretizations. The reason for such choice is based on the fact that the circumference $P(k)$ of the Cayley tree (i.e. the number of outer vertices located at the distance k from the tree root) grows as $P(k) = z \times z^{k-1}$, where z is the coordinational number of the Cayley tree ($z = 4$ for 4–branching tree). We shall assume that Cayley trees can cover the ”surface à godets” *isometrically*[‡], i.e. without gaps and selfintersections, preserving angles and distances—see figs.1b and 6a. Thus, our further aim consists in describing the relief of the ”surface à godets” in the 3–dimensional Euclidean space, under the condition that a regular 4–branching Cayley tree is isometrically embedded in this surface.

Comment.

Let us stress that in our paper we are interested in embedding of open (i.e. unbounded) surfaces only. From many textbooks on noneuclidean geometry we know that exponentially growing surfaces *with the boundary* can be isometrically embedded in a Euclidean space. The surface of revolution of the so-called *tractrix* around its asymptote is a famous example of such embedding [5]—see fig.2a. In 3D Euclidean space x, y, z the pseudosphere is

[†]The example of a 4–branching Cayley tree is considered for simplicity. In principle one can deal with any regular hyperbolic lattice. Some other examples are discussed at length of Section III.

[‡]For example, the rectangular lattice shown in fig.6b isometrically covers the Euclidean plane.

parametrized by the following equations:

$$\begin{cases} x = \cos u \sin v \\ y = \sin u \sin v \\ z = \cos v + \log \tan \frac{v}{2} \end{cases}$$

where $0 \leq u \leq 2\pi$ and $0 < v \leq \frac{\pi}{2}$.

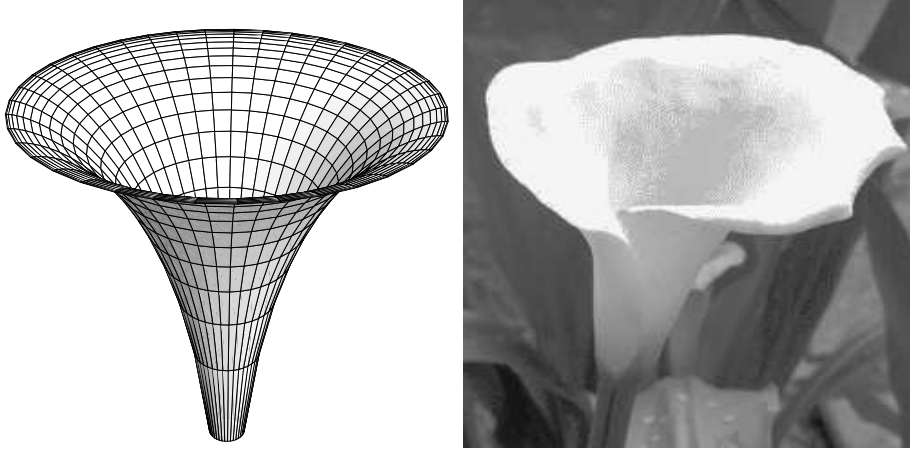


FIG. 2. (a) Pseudosphere, (b) Picture of calla lilly.

One sees from fig.2a that the surface of the pseudosphere has no crumples, and as it is bounded, it contains a *finite part* of a Cayley tree as an isometric embedding. We suspect that the pseudospheric structure can be also realized in the plants world. The picture of the flower of calla lilly reproduced in fig.2b supports our claim.

From our discussion, we conjecture that in the natural world both the surface à godets (SG) and the pseudosphere (PS) have equal rights to exist. From the biological point of view there is no difference between SG and PS—in both cases the same mechanism of cells proliferation is assumed. However from the topological point of view the very crucial point is the initial structure of the growing surface: if in the initial phase the growing structure is “pipe-like”, then one can expect the pseudosphere formation, while if the initial surface is almost flat and all circumference cells are independently growing, we ultimately arrive at a surface à godets.

After this comment we turn to the question of embedding isometrically a 4-branching *infinite* Cayley tree into a 2-manifold (“surface à godets”), viewed as an open surface in the 3D Euclidean space.

II. ISOMETRIC EMBEDDING OF A “SURFACE À GODETS” INTO THE 3D EUCLIDEAN SPACE

A. The model

Take a zero-angled rectangle $A_\zeta B_\zeta A'_\zeta C_\zeta$ bounded by arcs and lying in the unit disc $|\zeta| < 1$ as shown in fig.3d. Make reflections of the interior of the rectangle with respect to its sides $A_\zeta B_\zeta$, $B_\zeta A'_\zeta$, $A'_\zeta C_\zeta$, $C_\zeta A_\zeta$ and get a new generation of vertices – the new images of the initial zero-angled rectangle [6]. For example, the reflection with respect to the arc $A'_\zeta C_\zeta$ (which by definition remains unchanged) transforms $A_\zeta \rightarrow A''_\zeta$ and $B_\zeta \rightarrow B'_\zeta$.

Proceeding recursively with reflections, one isometrically tessellates the disc $|\zeta| < 1$ with all images of the rectangle $A_\zeta B_\zeta A'_\zeta C_\zeta$. If one connects the centers of neighboring (i.e. obtained by successive reflections) rectangles, one gets a 4-branching Cayley tree isometrically embedded into the unit disc endowed with the Poincaré metric [7] defined as follows:

$$ds^2 = \frac{d\zeta d\zeta^*}{(1 - \zeta \zeta^*)^2}$$

where ds is the differential length and the variables ζ and ζ^* are complex-conjugated.

It is known that the tessellation of the Poincaré disc by circular zero-angled rectangles is uniform in a surface of a 2-dimensional hyperboloid obtained by stereographic projection from the unit disc [5]. The open 2-hyperboloid is naturally embedded into a 3D space with *Minkovski metric*, i.e. with metric tensor of signature $\{+1, +1, -1\}$. However the problem of uniform embedding of an open 2-hyperboloid into a 3D space with *Euclidean metric* deserves special attention and exactly coincides with the main aim of our work—embedding of a 4-branching Cayley tree (isometrically covering the unit disc with Poincaré metric) into a 3D Euclidean space. Such embedding is realized by a transform $z = z(\zeta)$ which conformally maps a flat square $A_z B_z A'_z C_z$ in the complex plane z to a circular zero-angled rectangle $A_\zeta B_\zeta A'_\zeta C_\zeta$ in the unit disc $|\zeta| < 1$ (see fig.3). The relief of the corresponding surface is encoded in the so-called *coefficient of deformation* $J(\zeta) = \left| \frac{dz}{d\zeta} \right|^2$ coinciding with the Jacobian of the conformal transform $z(\zeta)$:

$$J(\zeta) = |z'(\zeta)|^2 = \begin{vmatrix} \frac{\partial \operatorname{Re} z}{\partial \operatorname{Re} \zeta} & \frac{\partial \operatorname{Re} z}{\partial \operatorname{Im} \zeta} \\ \frac{\partial \operatorname{Im} z}{\partial \operatorname{Re} \zeta} & \frac{\partial \operatorname{Im} z}{\partial \operatorname{Im} \zeta} \end{vmatrix}$$

Our final goal consists in an explicit construction of the function $J(\zeta)$.

Comments.

(A) The Jacobian $J(\zeta)$ has singularities ($J(\zeta) = \infty$) at all branching points—vertices $A_\zeta, B_\zeta, A'_\zeta, C_\zeta$ and their images.

(B) One can easily show that all the images of zero-angled rectangle $A_\zeta B_\zeta A'_\zeta C_\zeta$ in the complex plane ζ have the same area. Namely, the area of the elementary cell (the rectangle $A_z B_z A'_z C_z$) tessellating the plane z is

$$S = \int_{A_z B_z A'_z C_z} dz dz^*$$

Performing the transform $z(\zeta)$ one can rewrite S as follows

$$S = \int_{A_\zeta B_\zeta A'_\zeta C_\zeta} J(\zeta) d\zeta d\zeta^*$$

Taking into account the correspondence of boundaries under conformal transforms one arrives to the conclusion that all zero-angled rectangles have the same area S in ζ .

B. Construction of conformal maps

To find the conformal transform of the square $A_z B_z A'_z C_z$ in the z -plane to the zero-angled square $A_\zeta B_\zeta A'_\zeta C_\zeta$ in the ζ -plane, consider the following sequence of auxiliary conformal maps (shown in fig.3):

$$z \xrightarrow{z=z(w)} w \xrightarrow{w=w(\chi)} \chi \xrightarrow{\chi=\chi(\zeta)} \zeta$$

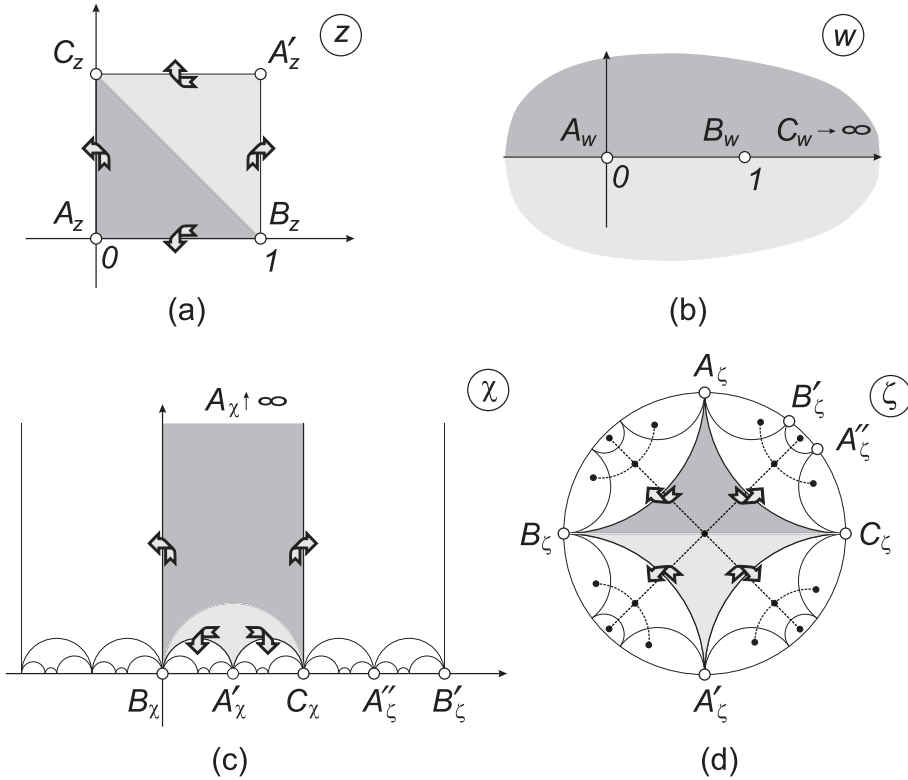


FIG. 3. Conformal maps: (a)–(b) $z = z(w)$; (b)–(c) $w = w(\chi)$; (c)–(d) $\chi = \chi(\zeta)$; (d) The Cayley tree isometrically covering the Poincaré disc $|\zeta| < 1$ is shown by dotted line.

Explicit construction of the functions $z(w)$, $w(\chi)$ and $\chi(\zeta)$ is described below.

1. The function $z = z(w)$ conformally maps the interior of the triangle $A_z B_z C_z$ with angles $\frac{\pi}{4}, \frac{\pi}{4}, \frac{\pi}{2}$ in the plane z onto the upper half-plane w (see fig.3a). The conformal map $z = z(w)$ is performed via Christoffel-Schwartz integral [8]

$$z(w) = \int_0^w \frac{d\tilde{w}}{\tilde{w}^{1/2} (1 - \tilde{w})^{3/4}} \quad (1)$$

with the following correspondence of branching points (see fig.3a):

$$\begin{cases} A_z(z = 0) \rightarrow A_w(w = 0) \\ B_z(z = 1) \rightarrow B_w(w = 1) \\ C_z(z = i) \rightarrow C_w(w = \infty) \end{cases}$$

2. The function $w = w(\chi)$ conformally maps the upper half-plane $\text{Im } w > 0$ to the interior of a circular triangle $A_\chi B_\chi C_\chi$ with angles $(0, 0, 0)$ lying in the upper half-plane $\text{Im } \chi > 0$ as it is shown in fig.3b. The standard theory of automorphic functions answers the question of explicitly constructing the map $w = w(\chi)$ (see, for example, [9,10]).

Consider a function $u(w)$ satisfying the hypergeometric equation with three branching points at $w = \{0, 1, \infty\}$:

$$w(w-1)u''(w) + \{(\alpha + \beta + 1)w - \gamma\}u'(w) + \alpha\beta u(w) = 0 \quad (2)$$

where the coefficients α, β, γ are uniquely defined by the angles of the circular triangle ABC : $\{\mu_1\pi, \mu_2\pi, \mu_3\pi\}$:

$$\mu_1 = 1 - \gamma; \quad \mu_2 = \gamma - \alpha - \beta; \quad \mu_3 = \beta - \alpha$$

In our case $\mu_1 = \mu_2 = \mu_3 = 0$, hence

$$\alpha = \frac{1}{2}; \quad \beta = \frac{1}{2}; \quad \gamma = 1$$

The equation (2) has two linearly independent fundamental solutions $u_1(w)$ and $u_2(w)$ which can be expressed in terms of hypergeometric functions $F(\alpha, \beta, \gamma, z)$. For our particular choice of parameters α, β, γ eq.(2) belongs to so-called degenerate case, where:

$$\begin{aligned} u_1(w) &= F\left(\frac{1}{2}, \frac{1}{2}, 1, z\right) \\ u_2(w) &= iF\left(\frac{1}{2}, \frac{1}{2}, 1, 1 - z\right) \end{aligned} \quad (3)$$

Recall that the function $F(\alpha, \beta, \gamma, z)$ admits the following integral representation

$$F(\alpha, \beta, \gamma, z) = \frac{\Gamma(\gamma)}{\Gamma(\beta)\Gamma(\gamma - \beta)} \int_0^1 t^{\beta-1} (1-t)^{\gamma-\beta-1} (1-zt)^{-\alpha} dt$$

It is known [9–11] that the conformal map $\chi(w)$ of the interior of a circular triangle $A_\chi B_\chi C_\chi$ with angles $(0, 0, 0)$ lying in the upper half-plane $\text{Im } \chi > 0$ to the upper half-plane $\text{Im } w > 0$ can be written as the quotient of fundamental solutions $u_1(w)$ and $u_2(w)$:

$$\chi(w) = \frac{u_1(w)}{u_2(w)} = -i \frac{F\left(\frac{1}{2}, \frac{1}{2}, 1, z\right)}{F\left(\frac{1}{2}, \frac{1}{2}, 1, 1-z\right)} \quad (4)$$

The conformal map of the circular triangle $A_\chi B_\chi C_\chi$ to the upper half-plane $\text{Im } w > 0$ is mutually single-valued, thus the inverse function $\chi^{-1}(w)$ solves our problem. Inverting the function $\chi(w)$, (this inverse function satisfies a Schartzian equation, which can be solved in our case, as shown in [11] p.23), we get:

$$w(\chi) = \frac{\vartheta_2^4(0, e^{i\pi\chi})}{\vartheta_3^4(0, e^{i\pi\chi})} \quad (5)$$

The conformal transform (5) establishes the following correspondence of branching points:

$$\begin{cases} A_w(w=0) & \rightarrow A_\chi(\chi=\infty) \\ B_w(w=1) & \rightarrow B_\chi(\chi=0) \\ C_w(w=\infty) & \rightarrow C_\chi(\chi=1) \end{cases}$$

3. The function $\chi = \chi(\zeta)$ conformally maps the interior of the circular triangle $A_\chi B_\chi C_\chi$ in the upper half-plane $\text{Im } \chi > 0$ to the interior of a circular triangle $A_\zeta, B_\zeta, C_\zeta$ in the open unit disc $|\zeta| < 1$ (see fig.3c). It is realized via the fractional transform

$$\chi(\zeta) = \frac{1-i}{2} \frac{\zeta+1}{\zeta-i} \quad (6)$$

with the following correspondence of branching points:

$$\begin{cases} A_\chi(\chi=\infty) & \rightarrow A_\zeta(\zeta=i) \\ B_\chi(\chi=0) & \rightarrow B_\zeta(\zeta=-1) \\ C_\chi(\chi=1) & \rightarrow C_\zeta(\zeta=1) \end{cases}$$

Collecting eqs.(1), (5) and (6) we arrive at a composite conformal map

$$z(\zeta) = z\{w[\chi(\zeta)]\}$$

The Jacobian $J(\zeta)$ of the map $z(\zeta)$ reads

$$\begin{aligned} J(\zeta) &\equiv \left| \frac{dz(\zeta)}{d\zeta} \right|^2 = \left| \frac{dz(w)}{dw} \right|^2 \left| \frac{dw(\chi)}{d\chi} \right|^2 \left| \frac{\chi(\zeta)}{d\zeta} \right|^2 \\ &= \frac{4}{\pi^2 |\zeta-i|^4} \left| \vartheta_1' \left(0, e^{i\pi \frac{1-i}{2} \frac{\zeta+1}{\zeta-i}} \right) \right|^2 \left| \vartheta_2 \left(0, e^{i\pi \frac{1-i}{2} \frac{\zeta+1}{\zeta-i}} \right) \right|^2 \end{aligned} \quad (7)$$

where (see [12])

$$\begin{aligned}\vartheta_1(\tau, e^{i\pi x}) &= 2e^{i\frac{\pi}{4}x} \sum_{n=0}^{\infty} (-1)^n e^{i\pi n(n+1)x} \sin(2n+1)\tau \\ \vartheta_1'(0, e^{i\pi x}) &\equiv \left. \frac{\vartheta_1(\tau, e^{i\pi x})}{d\tau} \right|_{\tau=0} = 2e^{i\frac{\pi}{4}x} \sum_{n=0}^{\infty} (-1)^n (2n+1) e^{i\pi n(n+1)x} \\ \vartheta_2(0, e^{i\pi x}) &= 2e^{i\frac{\pi}{4}x} \sum_{n=0}^{\infty} e^{i\pi n(n+1)x}\end{aligned}$$

C. Geometric structure of the leaf's boundary

Let us parameterize the "coefficient of deformation" $J(\eta) \equiv J(\eta, \varphi)$ by the variables (η, φ) , where η and φ are correspondingly the hyperbolic distance and the polar angle in the unit disc:

$$\eta = \ln \frac{1 + |\zeta|}{1 - |\zeta|}; \quad \varphi = \arctan \frac{\text{Im } \zeta}{\text{Re } \zeta}$$

Few sample plots of the function $J(\eta, \varphi)$ for $0 \leq \eta \leq \eta_{\max}$ and $0 \leq \varphi \leq \frac{\pi}{2}$ for $\eta_{\max} = 1.1; 1.4; 1.7$ are shown in fig.4a–c.

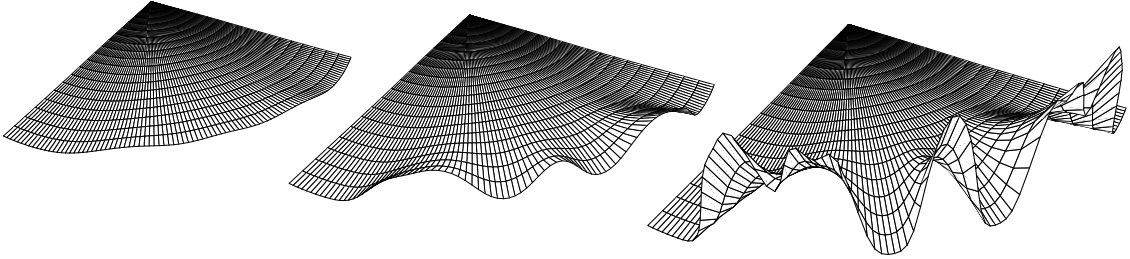


FIG. 4. Sample plots of $J(\eta, \varphi)$ for $0 \leq \eta \leq \eta_{\max}$ and $0 \leq \varphi \leq \frac{\pi}{2}$: (a) $\eta_{\max} = 1.1$; (b) $\eta_{\max} = 1.4$; (c) $\eta_{\max} = 1.7$.

Equation (7) solves the problem of embedding a "jupe à godets" isometrically covered by a 4-branching Cayley tree into the three-dimensional Euclidean space. The corresponding boundary profile is shown in fig.4.

The growth of the perimeter $P(\eta)$ of the circular "surface à godets" of hyperbolic radius η as well as the span $h(\eta)$ of transversal fluctuations can be characterized by the coefficients of growth ("Lyapunov exponents"), c_P and c_h defined as follows

$$c_P \equiv \lim_{\eta \rightarrow \infty} c_P(\eta) = \lim_{\eta \rightarrow \infty} \frac{\ln P(\eta)}{\eta}; \quad c_h \equiv \lim_{\eta \rightarrow \infty} c_h(\eta) = \lim_{\eta \rightarrow \infty} \frac{\ln h(\eta)}{\eta}$$

where

$$P(\eta) = \int_0^{2\pi} \sqrt{1 + \left[\frac{dJ(\eta, \varphi)}{d\varphi} \right]^2} d\varphi$$

and

$$h(\eta) = \int_0^{2\pi} J(\eta, \varphi) d\varphi$$

The plots of the functions $c_P(\eta)$ and $c_h(\eta)$ are shown in fig.5.

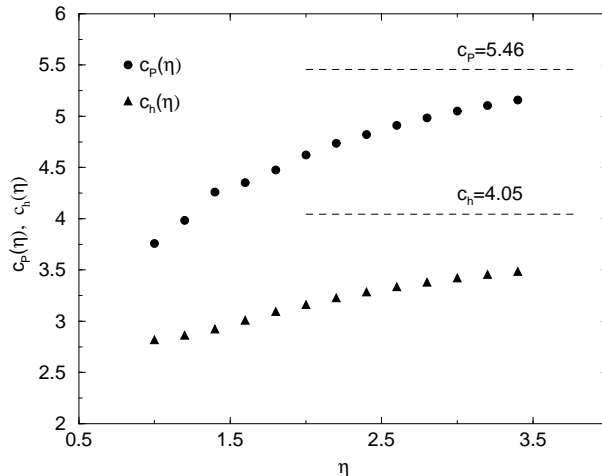


FIG. 5. Growth exponents $c_P(\eta)$ and $c_h(\eta)$.

III. GROWTH OF A RANDOM "SURFACE À GODETS"

The natural generalization of the model of a regular "surface à godets" defined in Section I consists in its "randomization". Suppose now that the growth phenomenon is random: extra area is generated only at randomly chosen ("active") sites. It means that in our model we insert extra triangles with probability $1 - q$ and leave an elementary domain unchanged with probability q . The vertices without inserted extra triangle we shall call "defects". They can be interpreted as defects of curvature, i.e. points where the surface is locally flat. It is easy to understand that if the probability of defects is $q = 0$, we return to the regular surface à godets with hyperbolic metric, while for $q = 1$ the resulting surface is flat (i.e. it can be embedded in a plane). We are interested in the dependence of the perimeter $P(k|q)$ on the radial distance k for the surface à godets with concentration of defects q .

Here again the problem becomes much more transparent if formulated for a discrete realization (isometrically embedded graph) of the "surface à godets". The issue is to define defects of curvature for graphs. First of all let us recall the definition of the Cayley graph of a group G .

By definition, the graph of the group G is constructed as follows:

- The vertices of the graph are labelled by group elements. Every element of the group is represented by some irreducible (i.e. written with the minimal number of letters) word (not necessarily unique) built from the letters – generators of the group G . Two words equivalent in the group G correspond to one and the same vertex of the graph.

- Two different vertices corresponding to nonequivalent words w and w' are connected by an edge (i.e. are nearest-neighbors) if and only if the word w' can be obtained from the word w by deleting one letter (generator of the group G), or adding one extra letter.

The following construction is of use.

1. It is known that a 4-branching Cayley tree is the graph of the *free* group Γ_2 (see fig.6a). The group Γ_2 is the infinite group of all possible words constructed from the set of letters $\{g_1, g_2, g_1^{-1}, g_2^{-1}\}$, where there are *no* commutation relations among the letters [6,13]. The total number of nonequivalent shortest (irreducible) words of length k in the group Γ_2 equals to the number $P_{\Gamma_2}(k)$ of distinct vertices of the 4-branching Cayley tree lying at a distance k from the origin (see fig.6a):

$$P_{\Gamma_2}(k) = 4 \times 3^{k-1} \quad (k \geq 1) \quad (8)$$

2. Consider now the opposite case of the *completely commutative* group E_2 . This group is generated by $\{f_1, f_2, f_1^{-1}, f_2^{-1}\}$, with the relation $f_1 f_2 = f_2 f_1$. The graph of the group E_2 is a 4-vertex lattice isometrically covering the Euclidean plane (see fig.6b). The problem of comparing two words w_1 and w_2 in the group E_2 written in different ways has a very straightforward solution. Taking into account that all generators of the group E_2 commute, we may write all irreducible words of length k in an *ordered form*:

$$w = g_1^{m_1} g_2^{m_2} \quad (|m_1| + |m_2| = k)$$

where

$$\begin{aligned} m_1 &= \#[\text{number of generators } f_1] - \#[\text{number of generators } f_1^{-1}] \\ m_2 &= \#[\text{number of generators } f_2] - \#[\text{number of generators } f_2^{-1}] \end{aligned}$$

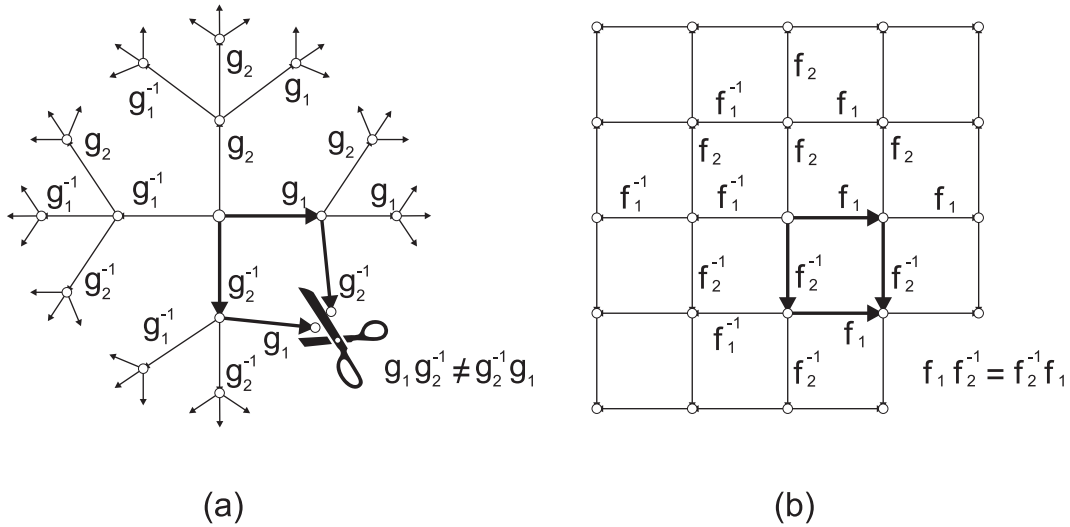


FIG. 6. (a) The 4-branching Cayley graph; (b) The graph (lattice) covering a surface with Euclidean (flat) metric.

It is convenient to encode the growth of the number of irreducible words with their length by an “incident matrix” \hat{T} . This construction relies on the automatic structure (see [14]) of the groups under consideration. All words of length $k + 1$ are obtained by right hand multiplication of words of length k by admissible generators. The admissible generators for a word w depend *only* on the last letter of w . In our case the entry (i, j) of the matrix \hat{T} is 1 if f_j is admissible after f_i and 0 otherwise. Let us note that the corresponding construction has been used recently in [15] in the case of ”locally free groups”. For the commutative group E_2 the incident matrix reads:

$$\hat{T} = \begin{array}{c|cccc} & f_1 & f_2 & f_1^{-1} & f_2^{-1} \\ \hline f_1 & 1 & 1 & 0 & 1 \\ f_2 & 0 & 1 & 0 & 0 \\ \hline f_1^{-1} & 0 & 1 & 1 & 1 \\ f_2^{-1} & 0 & 0 & 0 & 1 \end{array} \quad (9)$$

The total number of shortest words of length k is

$$P(k) = \mathbf{v} [\hat{T}]^{k-1} \mathbf{v}^\top = 4k \quad (k \geq 1) \quad (10)$$

where $\mathbf{v} = (1, 1, 1, 1)$ and \mathbf{v}^\top is the transposed vector.

Our idea to mimic the “surface à godets” with defects of curvature consists in the following. Let us insert “defects” in the commutation relations of the free group Γ_2 . It means that passing “along a word”, each time one meets a pair of consecutive generators with different subscripts (2 and 1), one either commutes them with probability q , or leave the sequence without changes with probability $1 - q$. The similar idea has been developed in [16] to approximate braid groups. More explicitly, one makes the following substitutions:

$$\begin{aligned} g_2 g_1 &\rightarrow \begin{cases} g_1 g_2 & \text{with prob. } q \\ g_2 g_1 & \text{with prob. } 1 - q \end{cases} ; & g_2^{-1} g_1 &\rightarrow \begin{cases} g_1 g_2^{-1} & \text{with prob. } q \\ g_2^{-1} g_1 & \text{with prob. } 1 - q \end{cases} \\ g_2 g_1^{-1} &\rightarrow \begin{cases} g_1^{-1} g_2 & \text{with prob. } q \\ g_2 g_1^{-1} & \text{with prob. } 1 - q \end{cases} ; & g_2^{-1} g_1^{-1} &\rightarrow \begin{cases} g_1^{-1} g_2^{-1} & \text{with prob. } q \\ g_2^{-1} g_1^{-1} & \text{with prob. } 1 - q \end{cases} \end{aligned} \quad (11)$$

For $q = 0$ we recover the commutation relations of the free group Γ_2 with exponentially growing ”volume” (the number of nonequivalent words) $P_{\Gamma_2}(k|q = 1)$, while for $q = 1$ we arrive at the group E_2 whose ”volume” $P_{E_2}(k|q = 1)$ displays a polynomial growth in k . Thus,

$$\begin{aligned} v_{\Gamma_2} &\equiv v(q = 0) = \lim_{k \rightarrow \infty} \frac{\ln P_{\Gamma_2}(k|q = 0)}{k} = \ln 3 > 0 \\ v_{E_2} &\equiv v(q = 1) = \lim_{k \rightarrow \infty} \frac{\ln P_{E_2}(k|q = 1)}{k} = 0 \end{aligned}$$

Let us insert ”defects” in commutation relations of the incident matrix $\hat{T}(x_1, \dots, x_4)$:

$$\hat{T}(x_1, \dots, x_4) = \begin{array}{|c|c|c|c|c|} \hline & g_1 & g_2 & g_1^{-1} & g_2^{-1} \\ \hline g_1 & 1 & 1 & 0 & 1 \\ \hline g_2 & x_1 & 1 & x_2 & 0 \\ \hline g_1^{-1} & 0 & 1 & 1 & 1 \\ \hline g_2^{-1} & x_3 & 0 & x_4 & 1 \\ \hline \end{array} \quad (12)$$

where

$$x_m = \begin{cases} 0 & \text{with probability } q \\ 1 & \text{with probability } 1 - q \end{cases} \quad (13)$$

and x_m are independent for all $1 \leq m \leq 4$.

The function $P(k|x_1^{(1)}, \dots, x_4^{(1)}, \dots, x_1^{(k)}, \dots, x_4^{(k)})$ describing the volume growth in an ensemble of words with random commutation relations, reads now (compare to (10))

$$P(k|x_1^{(1)}, \dots, x_4^{(1)}, \dots, x_1^{(k)}, \dots, x_4^{(k)}) = \mathbf{v} \left[\prod_{i=1}^{k-1} \hat{T}(x_1^{(i)}, \dots, x_4^{(i)}) \right] \mathbf{v}^\top \quad (14)$$

We shall distinguish between two distribution of defects: (a) annealed and (b) quenched. In case (a) the partition function $P(k|x_1^{(1)}, \dots, x_4^{(1)}, \dots, x_1^{(k)}, \dots, x_4^{(k)})$ is averaged with the measure (13), while in case (b) the "free energy", i.e. the logarithmic volume $v \sim \ln P$ is averaged with the same measure.

In the rest of the paper we pay attention to the case (a) only. Averaging the function $P(k|x_1^{(1)}, \dots, x_4^{(1)}, \dots, x_1^{(k)}, \dots, x_4^{(k)})$ over the disorder we get

$$P(k|q) \equiv \langle P(k|x_1^{(1)}, \dots, x_4^{(1)}, \dots, x_1^{(k)}, \dots, x_4^{(k)}) \rangle = \mathbf{v} \langle \hat{T}(x_1, \dots, x_4) \rangle^{k-1} \mathbf{v}^\top \quad (15)$$

where

$$\begin{aligned} \langle \hat{T}(x_1, \dots, x_4) \rangle &= \sum_{x_1=0}^1 \dots \sum_{x_4=0}^1 q^{4-(x_1+x_2+x_3+x_4)} (1-q)^{x_1+x_2+x_3+x_4} \hat{T}(x_1, x_2, x_3, x_4) \\ &= \begin{pmatrix} 1 & 1 & 0 & 1 \\ 1-q & 1 & 1-q & 0 \\ 0 & 1 & 1 & 1 \\ 1-q & 0 & 1-q & 1 \end{pmatrix} \end{aligned} \quad (16)$$

The highest eigenvalue λ_{\max} of the averaged matrix $\langle \hat{T}(x_1, \dots, x_4) \rangle$ defines the logarithmic volume $v^a(q) = \lim_{k \rightarrow \infty} \frac{\ln P(k|q)}{k}$ of the system with "annealed" defects in commutation relations:

$$v^a(q) = \ln \left(1 + 2\sqrt{1-q} \right) \quad (17)$$

One can check that for any $0 \leq q < 1$ the system is characterized by an exponential growth, i.e. $v^a(q) > 0$. However at $q = q_{cr} = 1$ one has a transition to a flat metric with $v^a(q = 1) = 0$. Expanding $v^a(q)$ in the vicinity of the transition point $q_{cr} = 1$, one gets

$$v^a(q)\Big|_{q \rightarrow 1^-} = 2(1-q)^{1/2} + O\left[(1-q)^{3/2}\right] \quad (18)$$

In the framework of the standard classification scheme, the phase transitions are distinguished by the scaling exponent α in the behavior of the free energy $F(\tau)$ near the critical point τ_{cr} [17]:

$$F(\tau)\Big|_{\tau \rightarrow \tau_{cr}} \propto |\tau_{cr} - \tau|^\alpha \quad (19)$$

Comparing (19) and (18) one can attribute (18) to a phase transition with the critical exponent $\alpha = \frac{1}{2}$.

IV. DISCUSSION

In Sections I and II we have developed a method based on conformal transforms allowing to describe the growth of a regular “jupe à godets”. Let us stress that our derivation is based on the assumption that the “jupe à godets” is isometrically covered by a 4-branching Cayley tree. We do not pretend to cover with this construction all possible surfaces à godets (let us recall that an exponentially growing structure like a “jupe à godets” has infinitely many discrete lattices of isometries), but to provide an analytical tool for a quantitative description of the main features of such surfaces. It would be in a sense more natural to suggest a construction, corresponding to another hyperlattice (so-called $\{3, 7\}$ -lattice [18]). Take the right hexagon consisting of 6 equal-sided triangles and make a radial cut along a side of one triangle as it is shown in fig.7. In a given cut insert an extra triangle such that the central point is surrounded now by 7 triangles; the resulting structure can be tentatively denoted as the “right 7-gon”. It is clear that such structure cannot be embedded in a plane anymore and has locally (near the center of a 7-gon) a saddle-like structure—see fig.7.

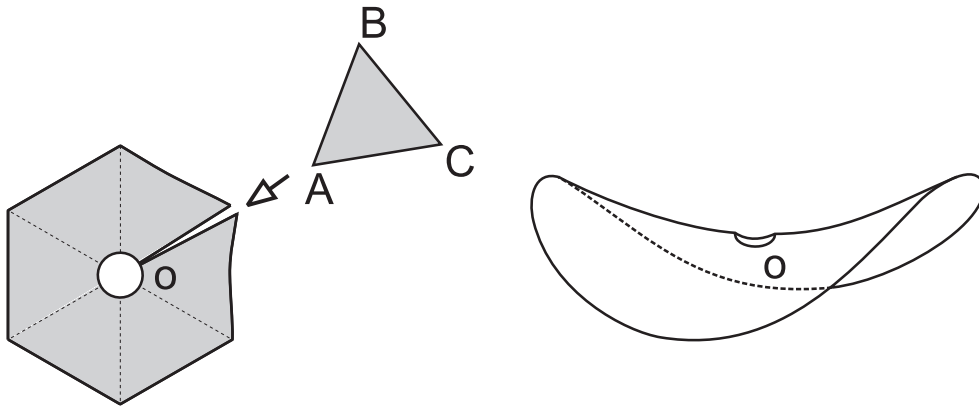


FIG. 7. A hexagon with a radial cut and inserted extra triangle and a saddle-like structure near the corner point.

Let us continue the surface construction and glue new equal-sided triangles to all perimeter bonds of a given 7-gon in such a way that each corner of any triangle in the surface is surrounded exactly by 7 triangles. Hence near each corner point the surface has a saddle-like structure. In what follows we shall call this structure the “7-gon surface à godets”.

Consider now the unit disc endowed with the hyperbolic Poincaré metric and take the equal-sided circular (i.e. bounded by geodesics) triangle ABC with angles $\left\{\frac{2\pi}{7}, \frac{2\pi}{7}, \frac{2\pi}{7}\right\}$ as shown in fig.8.

Make reflections of the interior of the triangle ABC with respect to its sides and get the images of the initial triangle, then make reflections of images with respect to their own sides and so on... In such a way one tessellates the whole disc by the images of the initial triangle ABC . It is easy to establish a topological bijection between the model of glued 7-gons and the system of hyperbolic triangles with angles $\left\{\frac{2\pi}{7}, \frac{2\pi}{7}, \frac{2\pi}{7}\right\}$, because all vertices are surrounded exactly by 7 curvilinear hyperbolic triangles—see fig.8.

The structure shown in fig.8 is invariant under conformal transforms of the Poincaré disc onto itself

$$\zeta \rightarrow \frac{\zeta - \zeta_0}{\zeta \zeta_0^* - 1}$$

where ζ and ζ^* are complex-conjugated and ζ_0^* is the coordinate of any image of the point 0 (vertex A of triangle ABC). Such conformal transform allows to shift any image of a vertex of any triangle to the center 0 of the disc (hence, such conformal transform replaces translations in Euclidean geometry).

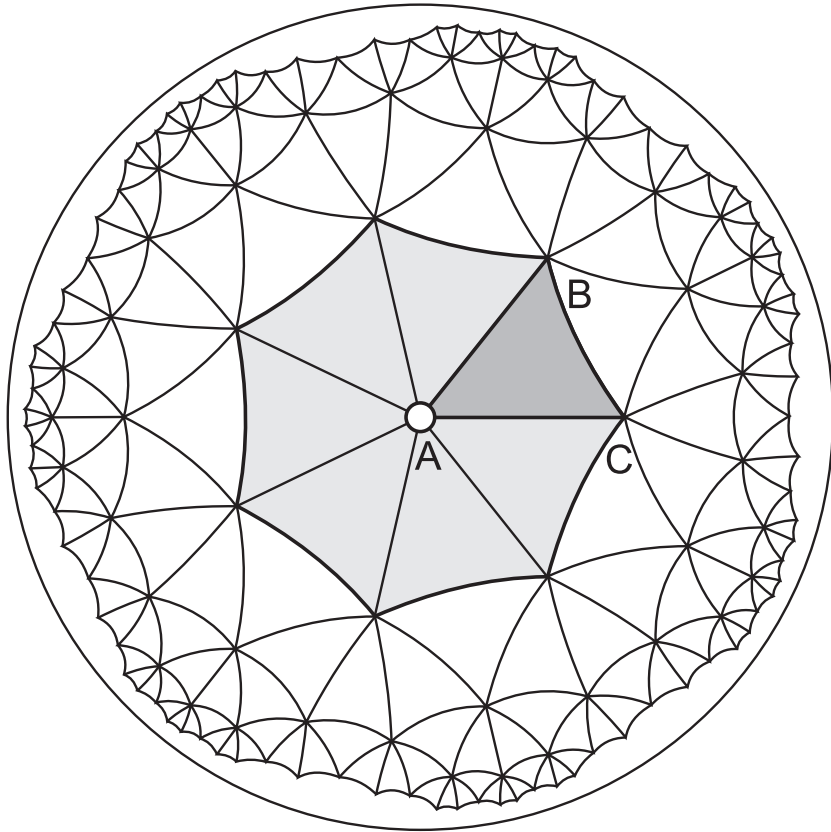


FIG. 8. A tessellation of a Poincaré disc by triangles with angles $\left\{\frac{2\pi}{7}, \frac{2\pi}{7}, \frac{2\pi}{7}\right\}$.

It would be desirable to develop the symbolic language allowing to investigate statistical properties of a “surface à godets” with and without random “defects of curvature” for the structure shown in fig.8. We expect that the symbolic language similar to the one developed in Section III applied to the group of reflections of triangles with angles $\left\{\frac{2\pi}{7}, \frac{2\pi}{7}, \frac{2\pi}{7}\right\}$ would allow such generalization.

Let us conclude with the following remark. The conformal embedding of a “7-gon surface à godets” shown in fig.8 into a 3D Euclidean space can be algorithmically solved in the same way as it has been done for the 4-branching Cayley tree. However for the “7-gon surface” we cannot derive an explicit expression for the coefficient of deformation $J(\zeta)$ in a simple form (like in eq.(7)). We outline this construction following results of Section II. Let $\tilde{z}(\tilde{\zeta})$ be the conformal transform of the triangle $\tilde{A}_z\tilde{B}_z\tilde{C}_z$ with angles $\left\{\frac{\pi}{3}, \frac{\pi}{3}, \frac{\pi}{3}\right\}$ in the complex plane z to the triangle $\tilde{A}_\zeta\tilde{B}_\zeta\tilde{C}_\zeta$ with angles $\left\{\frac{2\pi}{7}, \frac{2\pi}{7}, \frac{2\pi}{7}\right\}$ in the Poincaré disc $|\zeta| < 1$. The Jacobian $J(\tilde{\zeta})$ solves the problem of isometric embedding of a “7-gon surface à godets” into the 3D Euclidean space. For the proper choice of parameters α, β, γ in (2) we can derive the fundamental solutions $u_1(w)$ and $u_2(w)$ (and, hence $\chi(w)$), however unfortunately we are unable to find the inverse function $w(\chi)$. An explicit expression for $J(\tilde{\zeta})$ is therefore out of reach so far.

Acknowledgments

The authors are grateful to Vladimir Zakharov for drawing their attention to the problem as well as to Alexander Grosberg and Nicolas Rivier for stimulating discussions.

-
- [1] Crocheting a surface that becomes more "curly" as it approaches the infinite edge, <http://www.ou.edu/oumathed/Non-Egeometry/hyperbolic2.html>
- [2] <http://www.massey.ac.nz/~rmclachl//pseudosphere/tchebyshev.html>
- [3] L.Bowers, Negatively curved graph and planar metrics with applications to type, Michigan Math. J., **45**, 1, (1998), 31
- [4] S.Duval, M.Tajine, Trees formalism for fractal description (poster), Fractal'97, in *Fractals in the natural and Applied Sciences*, Denver, Colorado, USA, p.474 (1997)
- [5] M.J.Greenberg *Euclidean and Non-Euclidean Geometries: Development and History* (New York: W.H.Freeman & Co., 1993); D.C.Royster, *Neutral and Non-Euclidean Geometries* (<http://www.math.uncc.edu/~droyster/math3181/notes/hyprgeom/hyprgeom.html>)
- [6] W.Magnus *Noneuclidean Tessellations and their Groups* (London: Acad.Press, 1974); A.F.Beardon *The Geometry of Discrete Groups* (Berlin: Springer-Verlag, 1983);
- [7] B.A.Dubrovin, S.P.Novikov, A.T.Fomenko *Modern Geometry* (Berlin: Springer-Verlag, 1986)
- [8] W.Koppenfels, F.Stallmann *Praxis der Konformen Abbildung* (Berlin: Springer, 1959)
- [9] V.V.Golubev *Lectures on Analytic Theory of Differential Equations* (Moscow: GITTL, 1950)
- [10] E.Hille *Analytic Function Theory*, 1-2 (Boston: Ginn & Co., 1962)
- [11] H.Bateman, A.Erdelyi *Higher Transcendental Functions* (New York: Mcgraw-Hill, 1953)
- [12] M.Abramowitz, I.Stegun *Handbook of mathematical functions with formulas, graphs, and mathematical tables* (New York: Dover, 1965)
- [13] F.Klein, R.Fricke *Vorlesungen über die Theorie der Elliptischen Modulfunktionen. 1-2* (New York: Johnson reprint, 1966)
- [14] R.Charney, Geodesic Automation and Growth Functions for Artin Groups of Finite Type, Math. Ann., **301** (1995), 307
- [15] A.Vershik, S.Nechaev, R.Bikbov, Statistical Properties of Locally Free Groups with Applications to Braid Groups and Growth of Random Heaps, Comm.Math.Phys., **212** (2000), 469
- [16] A.Comtet, S.Nechaev, Random Operator Approach for Word Enumeration in Braid Groups, J.Phys.A: Math.Gen, **31** (1998), 5609
- [17] L.D.Landau, E.M.Lifshits *Statistical Physics, Part I* (3rd edition, Oxford: Pergamon Press, 1980)
- [18] E.Swierczak, A.Guttman, Self-avoiding walks and polygons on non-Euclidean lattices, J.Phys.A: Math.Gen, **29** (1990), 7485